A probabilistic high cycle fatigue model applied to cast Al-Si alloys

I. Koutiri[1], D. Bellett[1], F. Morel[1,] and L. Augustins[2]

[1] LAMPA, Arts et Métiers ParisTech, Angers, France. Imade.Koutiri@ensam.eu
[2] PSA Peugeot Citroën, Route de Gisy, 78943 Vélizy-Villacoublay Cedex, Case courrier VV1415.

ABSTRACT. *In this work, the high cycle fatigue behavior of cast hypo-eutectic Al-Si alloys is investigated. It is observed that two different coexisting fatigue initiation mechanisms can occur in these materials depending on the presence of different microstructural heterogeneities (i.e. micro-shrinkage pores, Si particles, Fe-rich inter-metallics, DAS of the Al-matrix, etc).Firstly, an experimental study is presented, highlighting the coexistence of these two fatigue damage mechanisms and their dependence on the presence of different micro-structural heterogeneities. A probabilistic high cycle fatigue model, which has the capacity to describe these two mechanisms, is then presented. The model contains the same principal ingredients as the one developed by [1]. It uses a probabilistic framework to link the two different fatigue damage mechanisms, and can take into account the mean stress and the effect of a biaxial stress state.*

INTRODUCTION

Due to their favourable combination of physical and mechanical properties, cast aluminium alloys have received much use in the automobile industry. One example is the casting of aluminium cylinder heads for automobile engines. In order to ensure that these components conform to their required specifications, numerical modelling techniques are employed [2]. The results from these simulations show that certain zones of these components are subjected to complex multiaxial cyclic stress-stain states, including high mean stress. The development of an appropriate criterion, for this application, is the object of this work.

MATERIAL: AlSi7Cu05Mg03-T7 (A356-T7)

Fatigue specimens were made from material taken from cylinder heads, manufactured by PSA for use in diesel automobile engines. The resulting mechanical properties of the material are listed in Table 1. Figure 1~~Figure 1~~ shows the material microstructure. It is composed of alpha-phase dendrites with an average Dendrite Arm Spacing (DAS) of approximately 80 µm.

Mis en forme : Anglais (États Unis)

Table 1 - Mechanical properties of AlSi7Cu05Mg03-T7

0.2% Yield stress,	Ultimate tensile strength,	Percent elongation at rupture,
250 - 260 MPa	318 - 330 MPa	5.0 - 5.7 %

The eutectic silicon particles are fine and spherical. The dark feature in Figure 1~~Figure 1~~ is a casting defect (i.e. a micro-shrinkage pore).

Mis en forme : Anglais (États Unis)

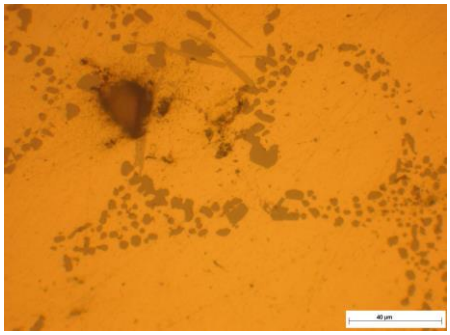

Figure 1. Microstructure of AlSi7Cu05Mg03

EXPERIMENTAL CONDITIONS – FATIGUE TESTS

Plane bending fatigue tests

All of the fatigue tests presented below were conducted at ambient temperature and pressure. A series of uniaxial plane bending fatigue tests were undertaken, with the aim of identifying the effect of the mean stress. Five different load ratios have been investigated: R = -1; R = 0.1; R = 0.62 (with the maximum stress slightly less than the yield stress, $\Sigma_{max} \approx \Sigma_Y$) ; R = 0.88 (with the mean stress equal to the yield stress, $\Sigma_m = \Sigma_Y$); R = 0.92 (with the maximum stress slightly less than the ultimate tensile strength, $\Sigma_{max} \approx \Sigma_{uts}$). For each load ratio, the fatigue strength at $2x10^6$ cycles was determined via the staircase method (10 specimens). All tests were done using a RUMUL Cracktronic electo-magnetic resonance fatigue testing machine. The test frequency was approximately 80 Hz.

Biaxial and Torsional fatigue tests

Torsional fatigue tests, with zero mean stress (R=-1), were also done. The RUMUL Cracktronic machine was used with the same testing conditions as described above.

An axisymmetrical bending testing apparatus was developed to undertake these Biaxial fatigue tests (see Figure 2~~Figure 2~~). This test setup forms the object of a French national patent submitted in May 2011 [3]. Disk shaped specimens with a reduction in thickness on the compressive side of the specimen are tested (see Figure 2~~Figure 2~~(b)). The tests were conducted using a servo-hydraulic INSTRON 8802 fatigue testing machine.

Mis en forme : Police :12 pt

Mis en forme : Police :12 pt

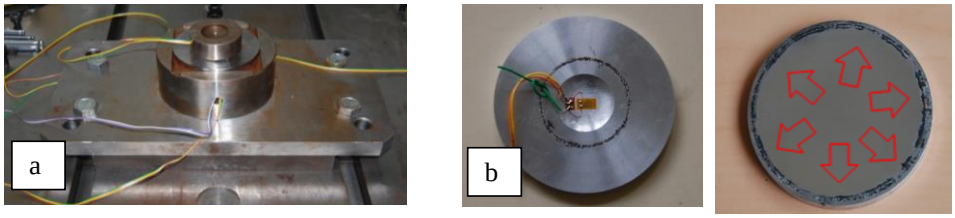

Figure 2. (a) An axisymmetrical bending testing apparatus for equibiaxial fatigue testing (b) Disk shaped test specimen (strain gauge shown on the compressive side)

Note that only positive load ratios can be tested using this setup, and that the equibiaxial stress state is proportional and in-phase. The equibiaxial fatigue limit at $2x10^6$ cycles has been determined for a load ratio of R=0.1 using the staircase method (with 9 specimens). The tests were conducted at a frequency of 20Hz.

FATIGUE BEHAVIOUR

The mean stress effect: AlSi7Cu05Mg03-T7

Table 2 summarises the uniaxial results in terms of the fatigue limits at $2x10^6$ cycles for 50% probability of failure.

Table 2. Uniaxial fatigue results

Plane Bending			
Σ_{moy} *(MPa)*	Σ_{amp} *(MPa)*	*Load Ratio*	*Standard deviation (MPa)*
0	82.5	-1	17.7
77	63.1	0.1	32.8
195.5	44.5	0.62	7
251	15	0.88	5.3
283.5	11.5	0.92	5.3

It is important to note that, even for the high load ratios (R = 0.88 and 0.92) a fatigue limit at $2x10^6$ cycles exists. These load ratios correspond to high mean stress and small stress amplitude, where the maximum stress is close to the ultimate tensile strength of the material.

The effect of an equibiaxial stress state

For the cast aluminium alloy in question, Figure 3~~Figure 3~~ shows the comparison between the uniaxial and equibiaxial fatigue test results for a load ratio of R=0.1.

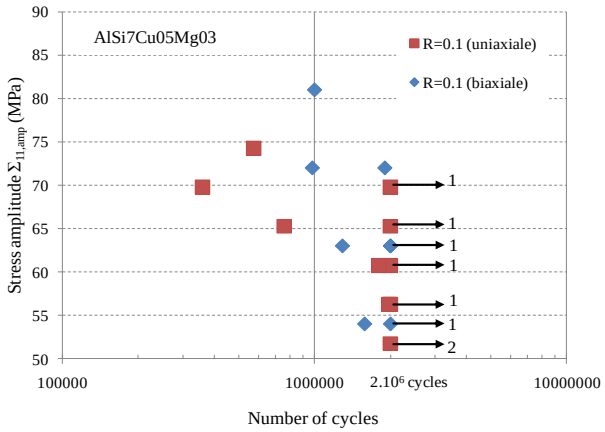

Figure 3. Wohler diagram for AlSi7Cu05Mg03 (R=0.1, plane bending: uniaxial stress state and R=0.1, axisymmetrical bending: equibiaxial stress state)

This diagram highlights the fact that the dispersion for both loading types is basically the same, and more surprisingly it shows that there is very little difference between the average fatigue limits at $2x10^6$ cycles. This implies that an equibiaxial loading condition does not result in greater fatigue damage than the uniaxial case (at least for this material).

FATIGUE DAMAGE MECHANISMS

Uniaxial loads

Fatigue crack initiation sites can be varied. However, when micro-shrinkage pores are present they play the fundamental role in controlling fatigue behaviour. When specific treatments, such as HIP (Hot Isostatic Pressing), are used to obtain a microstructure which is practically void of micro-shrinkage pores, crack initiation occurs at other microstructural heterogeneities [4, 5]. In this work, initiation of the fatigue crack resulting in final failure of the specimens almost always occurs at a micro-shrinkage pore (see Figure 4~~Figure 4~~).

It is therefore concluded that fatigue damage in this material is controlled by two different fatigue crack initiation mechanisms: One mechanism is associated with relatively large micro-shrinkage pores and the other is controlled by much smaller microstructural heterogeneities or the material matrix.

It is proposed that the first mechanism is basically a problem of crack propagation, or more precisely, of non-propagation (see Figure 5~~Figure 5~~b)). The second mechanism is assumed that crack initiation is controlled by localised plasticity.

Mis en forme : Police :12 pt, Anglais (États Unis)

Mis en forme : Police :12 pt, Anglais (États Unis)

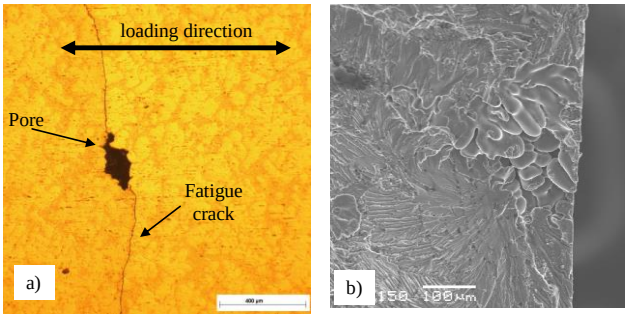

Figure 4. Fatigue crack initiation from a micro-shrinkage pore in AlSi7Cu05Mg03, loaded uniaxially with an R-ratio of R=-1 a) Surface observation b) SEM image of a failure surface

THE PROPOSED MODEL

The major advantage of the model proposed in this work is that both of these approaches are used. This approach uses the basic ingredients of the model proposed by Pessard and Morel [1] for the prediction of anisotropic fatigue behaviour of forged steels.

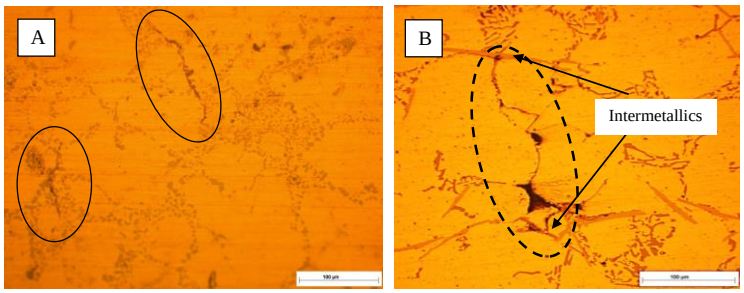

Figure 5. a) Fatigue crack initiation at Si-particles in the eutectic zones b) Initiation from a micro-shrinkage pore stopped by the presence of microstructural barriers

Modeling the fatigue damage occurring in the material matrix

The purpose of this section is to present the model used to describe the mechanism associated with the apparition of fatigue cracks in the material matrix, without the presence of micro-shrinkage pores. In order to estimate the probability of crack initiation, P_{F1}, due to the apparition of meso-plasticity in the material matrix, the Huyen and Morel [6] criterion is used. This approach is based on the hypothesis of elastic shakedown at the mesoscopic scale and the weakest link theory applied to all material planes of a R.E.V. The random character of the fatigue resistance is introduced via a Weibull distribution. The essential ingredients of this criterion are as follows. The probability of fatigue failure can be expressed as:

$$P_{F1} = 1 - exp\left[-\frac{1}{V_{01}}\int_V \frac{{X_a}^{m_1} I_{m1}}{{T_{01}}^{m_1}} dV\right] \quad (1)$$

Where $X_a = \max_{\theta,\phi,\psi}\{\chi_a(\theta,\phi,\psi)\}$ and $\chi_a(\theta,\phi,\psi) = T_a(\theta,\phi,\psi) + \alpha\Sigma_{n,a}(\theta,\phi)$ $T_a(\theta,\phi,\psi)$ is the shear stress amplitude in a direction defined by three angles (θ,ϕ,ψ), $\Sigma_{n,a}(\theta,\phi)$ is the amplitude of the normal stress acting on the material plane,m_1 is the Weibull exponent related to the scatter associated with the fatigue initiation mechanism To simplify the notation the parameter I_{m1} is introduced and is equal to:

$$I_{m1} = \int_{\phi=0}^{2\pi}\int_{\theta=0}^{\pi}\int_{\psi=0}^{2\pi}\left(\frac{\chi_a(\theta,\phi,\psi)}{\left(1-\gamma\Sigma_{n,m}(\theta,\phi)\right)X_a}\right)^{m_1} sin\theta d\theta d\phi d\varphi \quad (2)$$

$\Sigma_{n,m}(\theta,\phi)$ is the mean value of the normal stress acting on the material plane. The tripple integration in equation (2) is used to take into account the crack initiation potential on each possible slip system within an elementary volume. T_{o1} is the scale parameter of the Weibull distribution, α and γ are material parameters used to take into account the effect of the normal stress. It has been shown that this model results in good high cycle fatigue predictions for multiaxial loading conditions and in particular tension-torsion loads and biaxial loads [7].

Modelling the fatigue damage due to micro-shrinkage pores

The probability that a crack will propagate from a micro-shrinkage pore, P_{F2} is taken into account using concepts from Linear Elastic Fracture Mechanics. The micro-shrinkage pores are assumed to be pre-existing cracks for which mode I propagation is dominate. The range of the stress intensity factor ΔK can be estimated as a function of the applied stress range. The no-propagation condition is defined by comparing the stress intensity factor ΔK to the crack propagation threshold of the material, ΔK_{th}. It is therefore assumed that failure occurs if:

$$\Delta K \quad > \Delta K_{th} \quad (3)$$

The random nature of the crack propagation threshold is introduced using a Weibull distribution:

$$f_{02}(\Delta K_{th}) = \frac{m_2}{\Delta K_{th02}}\left(\frac{\Delta K_{th}}{\Delta K_{th02}}\right)^{m_2-1} exp\left[-\left(\frac{\Delta K_{th}}{\Delta K_{th02}}\right)^{m_2}\right] \quad (4)$$

Where m_2 is the Weibull exponent controlling the dispersion and ΔK_{th02} is the scale parameter associated with the damage mechanism. All cracks which are potentially active are taken into account via the calculation of $\Delta K(\theta,\varphi)$ on all possible material planes defined by the angles (θ,φ). In order to estimate the possibility of crack propagation, the weakest link hypothesis is applied to all plane of a reference volume V_0. The probability of crack propagations is thus given as:

$$P_{F02} = P\left(\Delta K_{th} < \Delta K(\theta,\varphi)\right) =$$
$$1 - exp\left[-\frac{1}{D_{02}}\int_{\varphi=0}^{2\pi}\int_{\theta=0}^{\pi}\left(\frac{\Delta K_{th}(\theta,\varphi)}{\Delta K_{th02}}\right)^{m_2} sin\theta d\theta d\varphi\right] \quad (5)$$

The probability of rupture, for the total volume of loaded material, can be obtained by apply the weakest link hypothesis a second time. So that:

$$P_{F2} = 1 - exp\left[-\frac{1}{V_{02}}\int_V \left\{\int_{\varphi=0}^{2\pi}\int_{\theta=0}^{\pi}\left(\frac{\Delta K(\theta,\varphi)}{\Delta K_{th02}}\right)^{m_2} sin\theta d\theta d\varphi\right\} dV\right] \quad (6)$$

Where the stress intensity factor associated with plane (θ, φ) can be written as a function of the stress normal to the plane $\Delta\sigma(\theta, \varphi)$ and the defect size, a:

$$\Delta K(\theta, \varphi) = \Delta\sigma(\theta, \varphi)\beta\sqrt{\pi a} \quad (7)$$

The mean stress effect on ΔK_{th} is generally associated with the concept of crack closure. The evolution of the threshold, as a function of the load ratio R, is introduced. .

$$\frac{\Delta K_{th}}{\Delta K_{th0}} = f(R) = \frac{(1-R)}{(1-\kappa R)} \quad (8)$$

Where ΔK_{th0} is crack propagation threshold for an R-ratio of R=0. The probability of rupture of the complete structure is therefore given by:

$$P_{F2} = 1 - exp\left[-\frac{1}{V_{02}}\int_V \left\{\int_{\varphi=0}^{2\pi}\int_{\theta=0}^{\pi}\left(\frac{\Delta\sigma_a(\theta,\varphi)\beta\sqrt{\pi a}}{\Delta K_{th02}}\right)^{m_2} sin\theta d\theta d\varphi\right\} dV\right] \quad (9)$$

It is possible to simplify the expression for $P_{F2}$by introducting the factor J_{m2} which is defined as: $J_{m2} = \int_{\varphi=0}^{2\pi}\int_{\theta=0}^{\pi}\left(\frac{\sigma_{n,a}(\theta,\varphi)}{\Sigma_{n,a}}\right)^{m_2} sin\theta d\theta d\varphi$ (10)

Where $\Sigma_{n,a} = \max_{\theta,\varphi}\{\sigma_a(\theta, \varphi)\}$.

The final expression becomes $P_{F2} = 1 - exp\left[-\frac{1}{V_{02}}\int_V \frac{{\Sigma_{n,a}}^{m_2} J_{m2}}{\Sigma_{02}(R)^{m_2}} dV\right]$

where $\Sigma_{02}(R) = \frac{\overline{\Sigma_d(R=0)}\frac{(1-R)}{(1-\kappa R)}}{\Gamma(1+1/m_2){J_{m2}}^{-1/m_2}}$ and Γ is the Euler function, defined as $\Gamma(t) = \int_0^\infty x^{t-1}e^{-x}dx$. $\overline{\Sigma_d}$ is the average experimentally determined fatigue limit. The spatial integration allows all potential propagation sites to be taken into account as well as to better account for multiaxial loading conditions.

The total probability of survival

The total probability of survival on the component is defined by again applying the hypothesis of the weakest link. It is obtained by multiplying the two survival probabilities from the two different observed mechanisms: $1 - P_F = (1 - P_{F1})(1 - P_{F2})$. The entire process can be represented in the form of a probabilistic Kitagawa type diagram, schematically shown in Figure 6~~Figure 6~~.a, which describes the competition between the two observed mechanisms

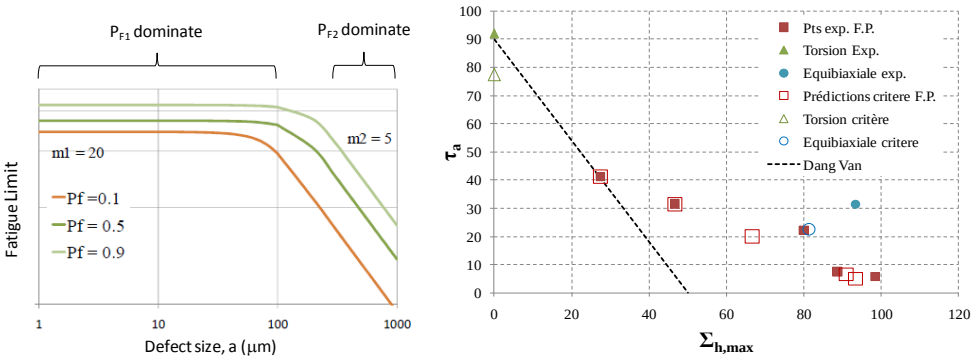

Figure 6. a.Schematic probabilistic Kitagawa type diagram and b.Dang Van diagram, showing the predictions of the proposed criterion

In order to compare the predictions of the proposed model with the experimental data presented above for different loading conditions (i.e. plane bending, axisymmetrical bending and torsion), the Dang Van criterion [8] is used. It can be seen that the predictions of the proposed criterion are in general less conservative and closer to the experimental data than the Dang Van criterion (figure 6.b).

CONCLUSIONS AND PROSPECTS

The principal objective of this work was to develop a probabilistic high cycle fatigue model adapted to Al-Si cast aluminum alloys, which is able to take into account the different microstructural heterogeneities present in the material. It has been concluded that two coexisting fatigue damage mechanisms occur in this material. In order to take into account both of these damage mechanisms, a probabilistic approach is used to model the "competition" between the two mechanisms. It is shown that the proposed model is capable of reproducing the experimentally observed tendencies, with respect to both the mean stress effect and the loading mode (torsion, uniaxial tension and equibiaxial tension). This work was undertaken in partnership with PSA Peugeot Citrooën and was financially supported by the French region, Pays de la Loire.

REFERENCES

1. Pessard E., Morel F., Morel A. and Bellett D., (2011), Modelling the role of non-metallic inclusions on the anisotropic fatigue behaviour of forged steel, International Journal of Fatigue, Vol. 33, pp. 568–577.
2. Comte F., Maclan N., Morin N., Maitournam H. and Moumni Z., (2005), Prise en compte des contrainte résiduelles de traitement thermique dans la prédiction de la tenue en service des culasses en aluminium, Proceedings of 17eme Congrès Français de Mécanique, Troyes, France Vol. 6 No 3, pp.343-348
3. Duparque C., Augustins L., Morel F. and Bellett D., (2011), Machine d'essai en fatigue biaxiale disposant d'une éprouvette, French Patent, submitted 17 May 2011, n° de demande 1154287, n° de soumission 1000112324.
4. Murali S., Arvind T.S., Raman K.S. and Smurthy K.S., (1997), Mater.Trans. JIM 38, 28.
5. Powell G.W., (1994), Mater. Charact. 33, 275.
6. Huyen Nguyen Thi Thu, (2008), Effet des hétérogéneités microstructurales sur le comportement en fatigue multiaxiale à grand nombre de cycles. PhD thesis. Arts et Métiers ParisTech Centre d'Angers LPMI.
7. Koutiri I., (2011), Effet des fortes contraintes hydrostatiques sur la tenue en fatigue des matériaux métalliques, PhD thesis. Arts et Métiers ParisTech Centre d'Angers LAMPA
8. Dang Van K., (1973), Sur la résistance à la fatigue des Métaux, Sciences et techniques de l'armement.